

DETAILED EXPERIMENTAL PROCEDURES

Cell Culture and Electrophysiology

Dissociated postnatal (P1-2) rat hippocampal neuron cultures, plated at a density of 230-460 mm² in poly-D-lysine-coated glass-bottom petri dishes (Mattek), were prepared as previously described (Sutton et al., 2006) and maintained for at least 21 DIV at 37 °C in growth medium [Neurobasal A supplemented with B27 and Glutamax-1 (Invitrogen)] prior to use. Whole-cell patch-clamp recordings were made with an Axopatch 200B amplifier from cultured hippocampal neurons bathed in HEPES-buffered saline (HBS; containing, in mM: 119 NaCl, 5 KCl, 2 CaCl₂, 2 MgCl₂, 30 Glucose, 10 HEPES, pH 7.4) plus 1 μM TTX and 10 μM bicuculine. Where indicated, some experiments used HBS containing (in mM) 1 CaCl₂ and 2 MgCl₂ or 0.5 CaCl₂ and 3.5 MgCl₂. Whole-cell pipette internal solutions contained, in mM: 100 cesium gluconate, 0.2 EGTA, 5 MgCl₂, 2 adenosine triphosphate, 0.3 guanosine triphosphate, 40 HEPES, pH 7.2, and had resistances ranging from 4-6 MΩ. Cultured neurons with a pyramidal-like morphology were voltage-clamped at -70 mV and series resistance was left uncompensated. mEPSCs were recorded in the presence of 1 μM TTX and 10 μM bicuculine and analyzed off-line using Synaptosoft mini analysis software. For paired-pulse facilitation experiments, HBS contained (in mM) 0.5 CaCl₂ and 3.5 MgCl₂ and evoked EPSCs were elicited with 0.3 ms pulses delivered by an extracellular bipolar stimulating electrode positioned near the recorded neuron. All PPF experiments were conducted within 15 min of CNQX or CNQX/TTX washout. Statistical differences between experimental conditions were determined by ANOVA and post-hoc Fisher's LSD test.

Immunocytochemistry and Microscopy

All imaging was performed on an inverted Olympus FV1000 laser scanning confocal microscope. Alexa 488 was excited with the 488 line of an argon ion laser and emitted light was typically collected between 500-530 nm with a tunable emission filter. Alexa 555/568 were excited with a 559 nm diode laser and emitted light was typically collected between 570-670 nm. Prior to image collection, the acquisition parameters for each channel were optimized to ensure a dynamic signal range and to ensure no signal bleed-through between detection channels. Identical acquisition parameters were used for each treatment condition, and in each experimental run, we verified that no detectable staining was observed in control samples incubated in the absence of primary antibody (but otherwise processed identically).

For BDNF staining, cells were treated in conditioned media as indicated, then fixed on ice for 30 min with 4% paraformaldehyde (PFA)/4% sucrose in phosphate buffered saline with 1 mM MgCl₂ and 0.1 mM CaCl₂ (PBS-MC), permeabilized (0.1 % Triton X in PBS-MC, 5 min), blocked with 2% bovine serum albumin (BSA) in PBS-MC for 30 min, and labeled with a rabbit polyclonal antibody against BDNF (Santa Cruz, 1:100) and a mouse monoclonal antibody against MAP2 (Sigma, 1:5000) for either 60 min at RT or overnight at 4°C. Alexa 488-conjugated goat anti-rabbit (1:250) and Alexa 555-cojugated goat anti-mouse (1: 1000) secondary antibodies (each 60 min at RT) were used to visualize BDNF and MAP2 staining, respectively. In a subset of experiments, Alexa 555-conjugated phalloidin (1:200, Molecular Probes) was used to identify dendritic processes in place of MAP2 staining. For experiments analyzing BDNF expression in axons and astrocytes, the BDNF staining described above was combined with direct Zenon Alexa 568 (Invitrogen) coupling to a Pan-axonal neurofilament mouse monoclonal antibody cocktail (1:8000, clone SMI-312, Covance) or a mouse monoclonal

antibody against GFAP (Sigma, 1:1000). Zenon labeling was conducted for 30-min following BDNF immunostaining, after which, the cells were lightly fixed (2% PFA, 5 min) to ensure stability of the signals over time. Neurons with a pyramidal-like morphology were selected for imaging by epifluorescent visualization of MAP2/phalloidin, neurofilament, or GFAP staining, to ensure blind sampling of BDNF expression. Analysis of BDNF expression in astrocytes, or somatic, dendritic, and axonal neuronal compartments was performed on maximal intensity z-compressed image stacks. In each case, BDNF expression was estimated by the average non-zero pixel intensity for each compartment. To analyze BDNF expression processes (axons, dendrites, and astrocytic processes), each process was linearized and extracted from the full-frame image using the straighten plugin for Image J. To combine data across multiple experimental runs of the same experiment, BDNF expression in each image was normalized against the average non-zero pixel intensity for the respective control group. Statistical differences were assessed by ANOVA, followed by Fisher's LSD post-hoc tests.

For analysis of surface GluR1 expression, neurons were live labeled with a rabbit polyclonal antibody recognizing a surface epitope of GluR1 (10 µg/ml; EMD Biosciences) for 15 min at 37 °C, followed by fixation (2 % PFA in PBS-MC for 15 min at RT), and immunocytochemical labeling with a mouse monoclonal anti-PSD95 antibody (1:1000; Chemicon) as described above. Alexa 488-conjugated goat anti-mouse (1:500) and Alexa 555-conjugated goat anti-rabbit (1:500) secondary antibodies (each 60 min at RT) were used to visualize PSD95 and GluR1 staining, respectively. Neurons were imaged with a Plan-Apochromat 63x/1.4 oil objective with 2x digital zoom and selected based on PSD95 epifluorescence to ensure blind sampling of surface GluR1. For analysis, "synaptic" GluR1 was defined as a particle that occupied greater than 10% of the area defined by a PSD95 particle, and

the average integrated intensity (total # of non-zero pixels * intensity) of synaptic GluR1 particles was calculated using custom written analysis routines for Image J. Analysis was performed on both full-frame images as well on dendrites that were straightened and extracted from the full-frame image, where “n” = the number of images or number of dendrites, respectively. Both analysis methods yielded similar results. Statistical differences were assessed by ANOVA, followed by Fisher’s LSD post-hoc tests.

To assess presynaptic function directly, we used live-labeling with an Oyster 550-conjugated rabbit polyclonal antibody against the luminal domain of synaptotagmin 1 (syt-lum; 1:100, Synaptic Systems). Prior to labeling, neurons were treated with 2 μ M TTX for 15 min to isolate spontaneous neurotransmitter release. Neurons were then labeled with anti-syt-lum for 5 min at RT, washed, fixed with 4% PFA/4% sucrose in PBS-MC, permeabilized and blocked as above, then labeled with either a mouse monoclonal antibody against bassoon (1:1000, Stressgen) or a guinea pig polyclonal anti-vglut1 antibody (1: 2500, Chemicon). The intrinsic fluorescent signal of the anti-syt-lum at synaptic sites was amplified by an Alexa 555-cojugated goat anti-rabbit (1:500) secondary antibody, while bassoon or vglut1 staining, respectively was visualized with an Alexa 635-cojugated goat anti-mouse (1:1:000) or Alexa 488-cojugated goat anti-guinea pig (1:250) secondary antibody (each for 60 min at RT). Neurons were imaged with a Plan-Apochromat 63x/1.4 oil objective with 2x digital zoom and selected based on vglut1 epifluorescence to ensure blind sampling of syt-lum expression. For analysis, a “synaptic” syt-lum particule was defined as a particle that occupied greater than 10% of the area defined by a vglut1 particle, and the proportion of vglut particles containing synaptic syt-lum particules was calculated using custom written analysis routines for Image J. Analysis was performed on both full-frame images as well on dendrites that were straightened and extracted from the full-frame

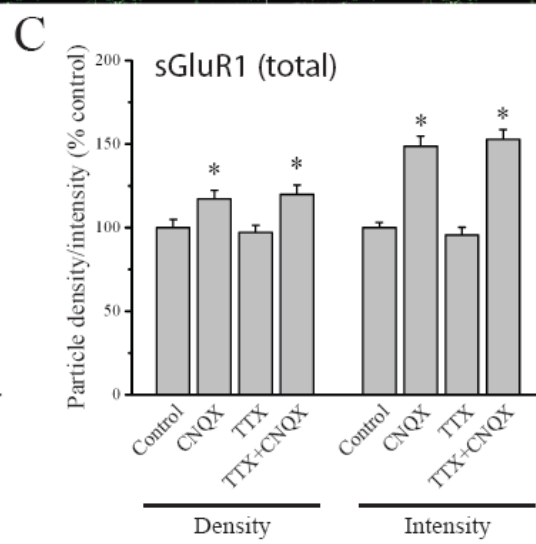
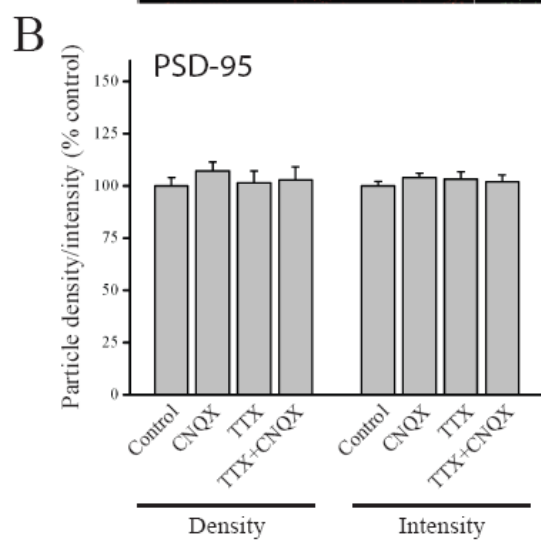
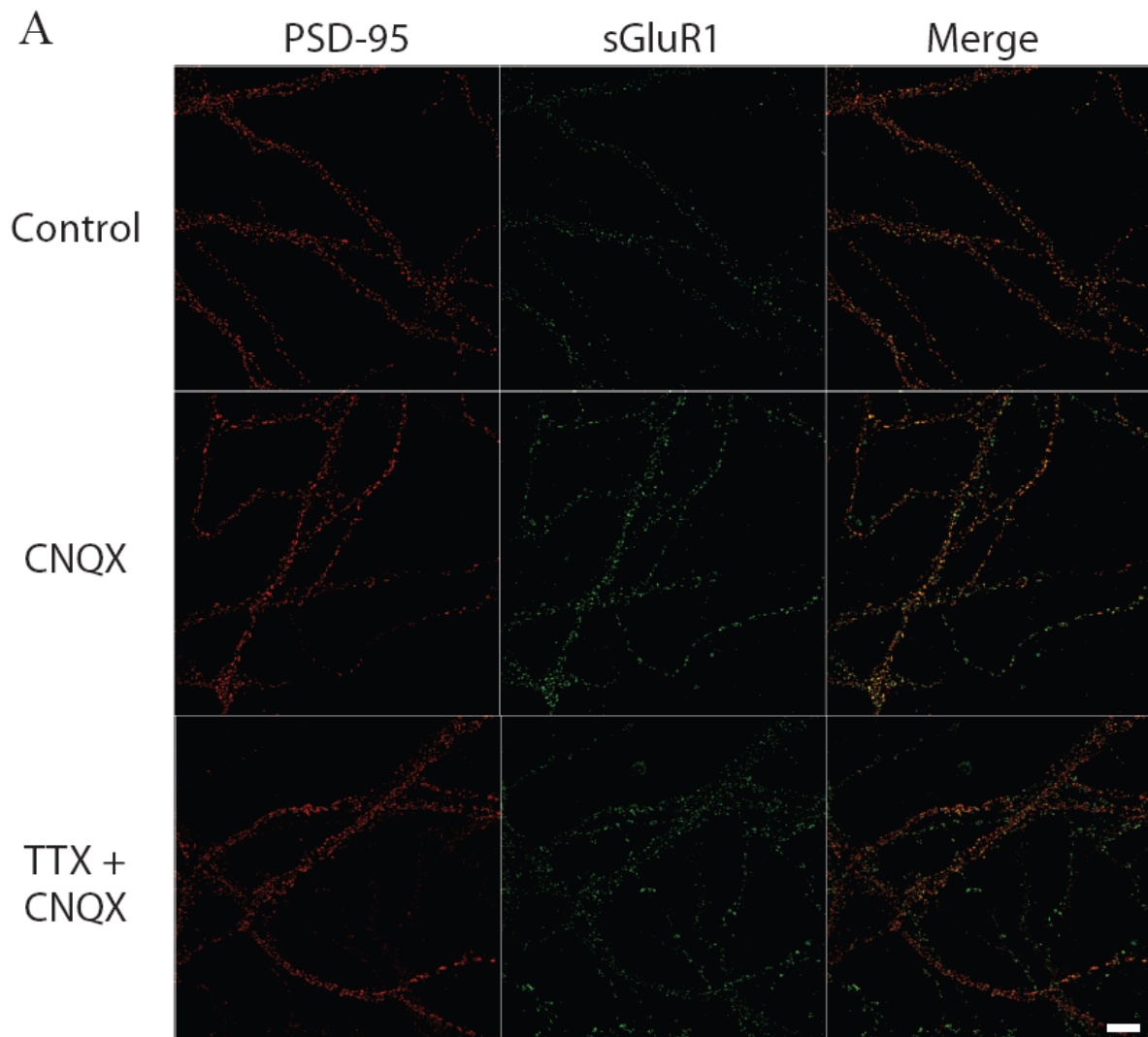
image, where “n” = the number of images or number of dendrites, respectively. The results from each analysis method were indistinguishable. Statistical differences were assessed by ANOVA, followed by Fisher’s LSD post-hoc tests.

Local Perfusion

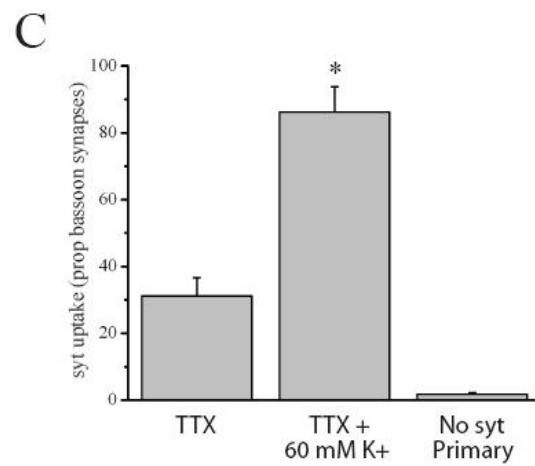
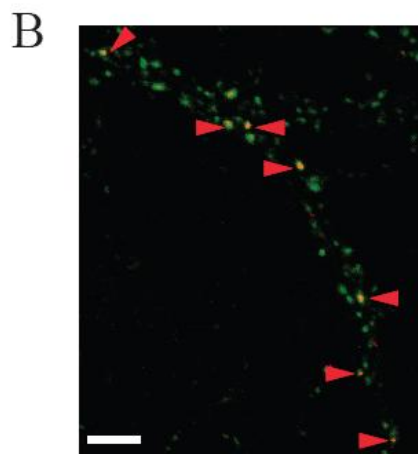
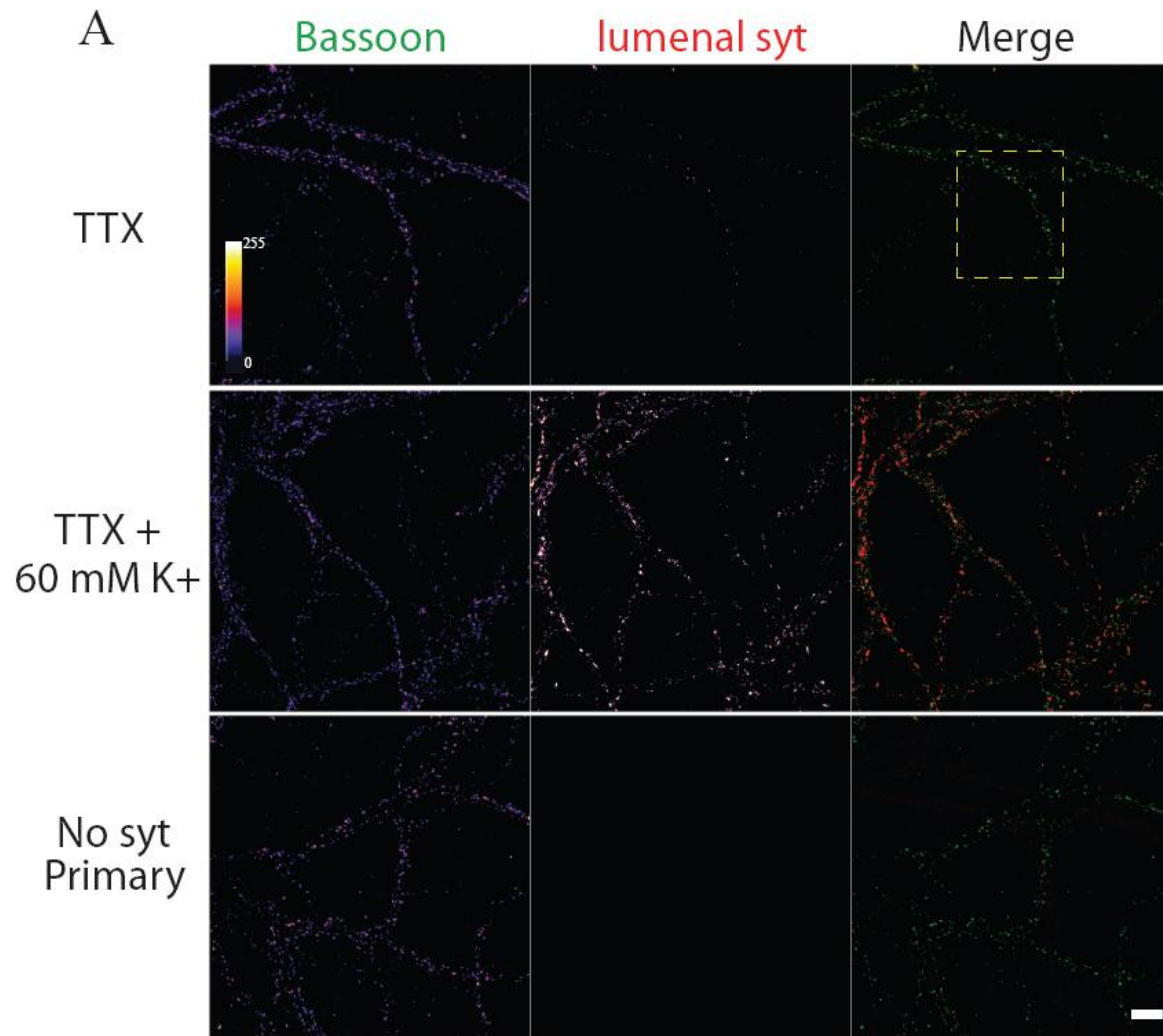
All local perfusion experiments were performed on an Olympus FV1000 laser- scanning confocal microscope using Plan-Apochromat 40x/0.95 air (for live imaging) and Plan-Apochromat 40x/1.0 oil (for retrospective imaging) objectives. Stable microperfusion was achieved by use of a dual micropipette delivery system, as described (Sutton et al., 2006). The delivery micropipette was pulled as a typical whole-cell recording pipette with an aperture of ~ 0.5 μm . The area of dendrite targeted for local perfusion was controlled by a suction pipette, which was used to draw the treatment solution across one or more dendrites and to remove the perfusate from the bath. A cell-impermeant fluorescent dye (either Alexa 488 or Alexa 555 hydrazide, 1 $\mu\text{g}/\text{ml}$) was included in the perfusate to visualize the affected area. In all local perfusion experiments, the bath was maintained at 37°C and continuously perfused at 1.5 ml/min with HBS.

For analysis, the size of the treated area was determined in each linearized dendrite based on Alexa 488/555 fluorescence integrated across all images taken during local perfusion. Adjacent non-overlapping dendritic segments, 25 μm in length, proximal (i.e., towards the cell soma) and distal to the treated area were assigned negative and positive values, respectively. For experiments examining local regulation of BDNF expression, cells were immediately fixed following local perfusion, and processed for immunostaining as described above. Analysis of BDNF expression in local perfusion experiments was performed on maximal intensity z-

compressed image stacks. The average non-zero pixel intensity for the entire length of dendrite, excluding the treated area, was used to normalize BDNF intensity and was assigned a value of 1. The intensity of BDNF immunofluorescence was then computed for the treated and all untreated dendritic segments and expressed relative to the average non-treated value. For experiments examining syt-lum uptake, immediately following local perfusion, 2 μ M TTX was bath applied for 10 min to isolate spontaneous neurotransmitter release. Neurons were then live labeled with anti-syt-lum for 5 min at RT, and processed for immunocytochemistry as described above. The density and intensity of vglut particles were calculated for each dendritic segment, and the average value in untreated segments was assigned a value of 1, which was then used to normalize vglut density and intensity in all segments (including the treated area). The proportion of vglut particles with syt-lum particles was also determined in each segment. Statistical differences in these measurements between segments were assessed by ANOVA and Fisher's LSD post-hoc tests.

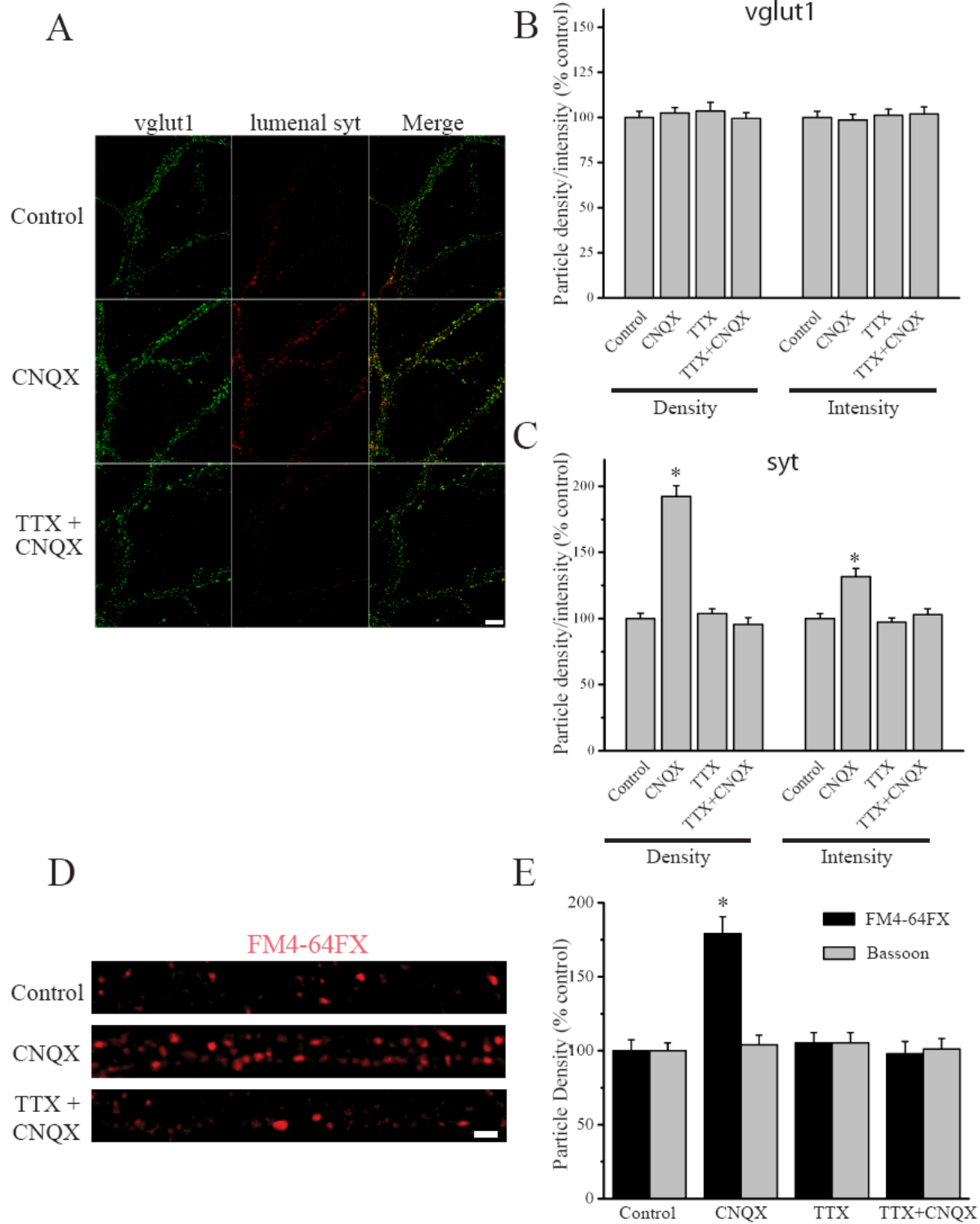


Supplementary Figure 1. Postsynaptic changes induced by AMPAR blockade are unaffected by coincident AP blockade. (A) Full-frame examples of PSD95 (left, red) and surface GluA1 (middle, green) staining from neurons (21-40 DIV) treated, as indicated; merged PSD95/sGluA1 images are shown in the right panel; scale bar = 10 μ m. (B) Mean (+SEM) normalized (relative to the average control value) density and intensity of PSD95 particles in the various treatment groups. (C) Mean (+SEM) normalized (relative to the average control value) density and intensity of surface GluA1 particles in the various treatment groups, irrespective of PSD95 colocalization. AMPAR blockade (CNQX) or AMPAR + AP blockade (TTX+CNQX) each produced significant (* $p < 0.05$, relative to control) increases in surface GluR1 expression without accompanying changes in PSD95 expression.



Jakawich et al. Figure S2.

Supplementary Figure 2. Activity-dependent uptake of syt-lum at synapses. Neurons (21-40 DIV) were live-labeled with a rabbit polyclonal antibody against the luminal domain of synaptotagmin 1 for 5 min in the presence of 2 μM TTX in either normal HBS or HBS with 60 mM K^+ (equimolar KCL-NaCl substitution), fixed, and processed for immunostaining against bassoon (a structural synaptic marker). (A) Full-frame examples of Bassoon (left, green) and luminal synaptotagmin (middle, red) staining from neurons treated, as indicated; merged bassoon (green) and syt (red) images are shown in the right panel; fluorescence intensity given by color look-up table; scale bar = 10 μm . Direct depolarization (60 mM K^+) of presynaptic terminals markedly enhances syt-lum uptake, demonstrating the activity-dependent nature of syt-lum staining. While weaker, labeling in the presence of TTX and normal K^+ is still specific and synaptic. (B). Higher magnification view of the area marked by a dashed box in (A), illustrating strong colocalization (red arrowheads) between syt uptake and bassoon staining; scale bar = 5 μm . (C). Mean (+ SEM) percentage of bassoon-positive synapses with syt-lum labeling in the indicated conditions. Direct terminal depolarization significantly ($*p < 0.05$, relative to TTX alone) enhances syt-lum uptake.

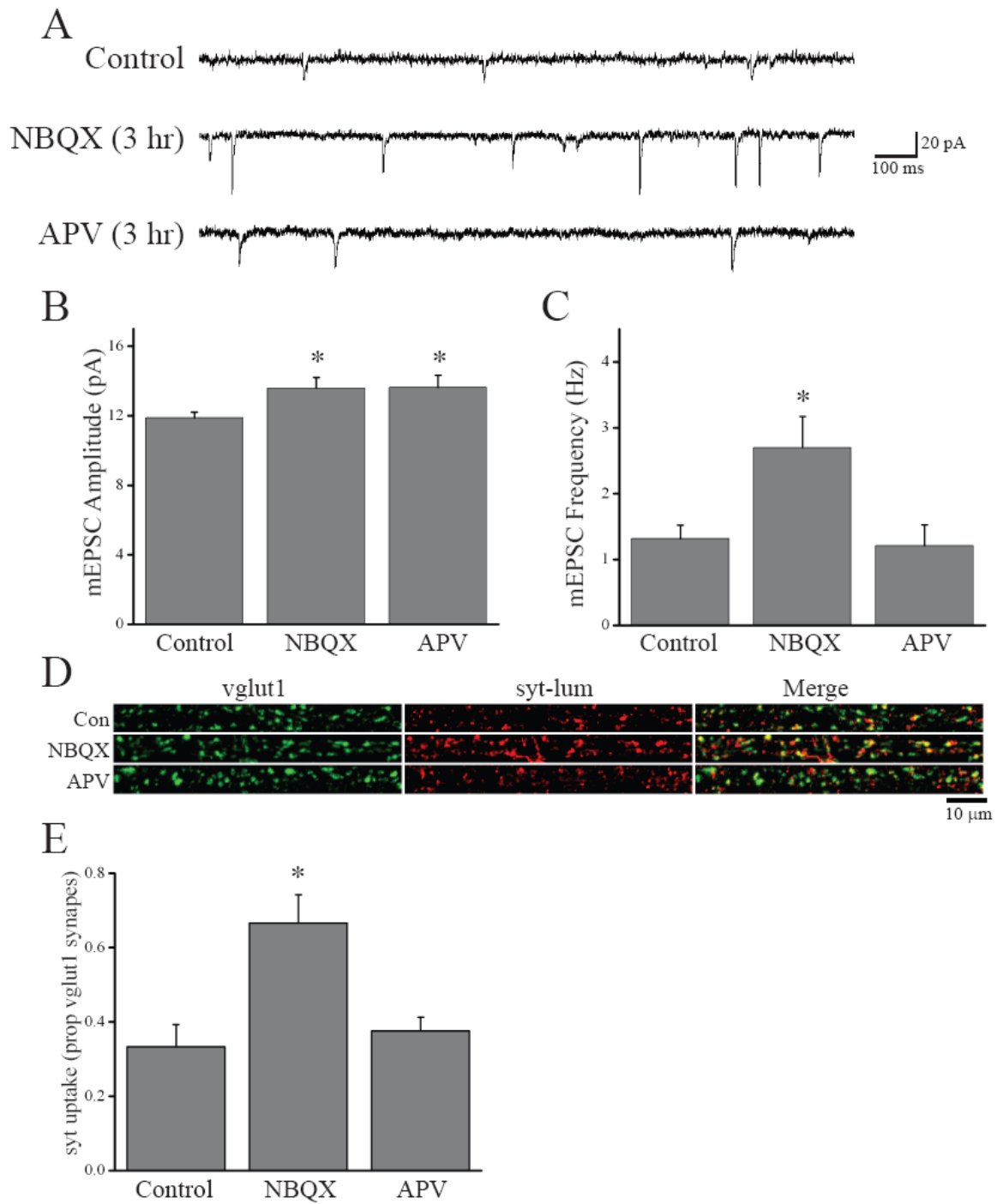


Jakawich et al. Figure S3.

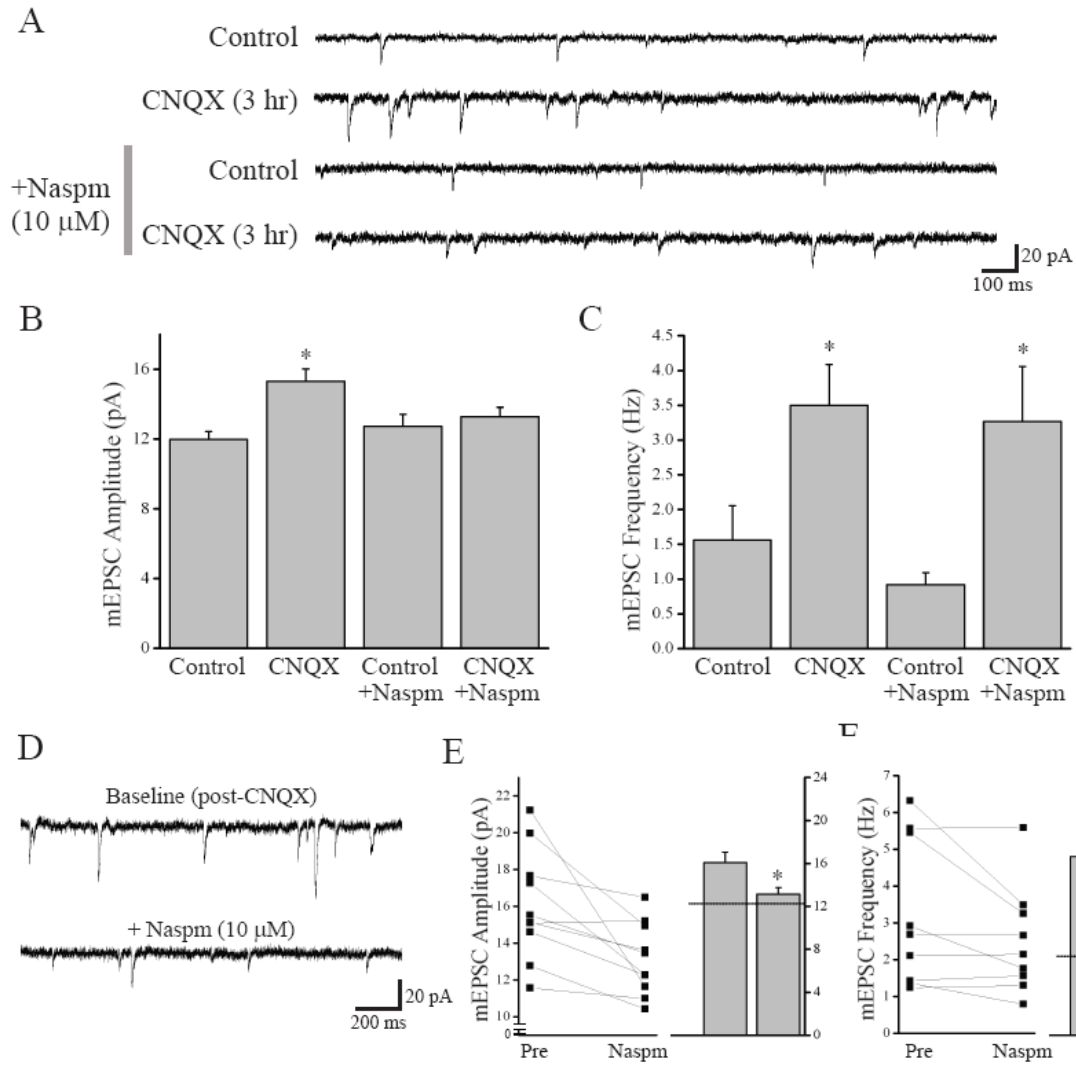
Supplementary Figure 3. Presynaptic changes induced by AMPAR blockade are prevented

by coincident AP blockade. (A) Full-frame examples of vglut1 (left, green) and syt-lum (middle, red) staining from neurons (21-40 DIV) treated, as indicated; merged vglut1/syt-lum images are shown in the right panel; scale bar = 10 μm . (B) Mean (+SEM) normalized (relative to the average control value) density and intensity of vglut1 particles in the various treatment groups. (C) Mean (+SEM) normalized (relative to the average control value) density and intensity of syt-lum particles in the various treatment groups, irrespective of vglut1 colocalization. AMPAR blockade (CNQX) significantly ($*p < 0.05$, relative to control) enhanced syt-lum uptake, without changes in overall excitatory synapse density; these changes were prevented by coincident AP blockade (TTX+CNQX). (D) Representative linearized examples of FM4-64FX staining in control neurons or those deprived of activity for 3 hrs via either AMPAR blockade alone (40 μM CNQX), AP blockade alone (2 μM TTX), or both AMPAR + AP blockade (TTX+CNQX); scale bar = 2 μm . Prior to labeling, neurons in all treatment conditions were treated with 2 μM TTX in HBS for 10 min to isolate spontaneous neurotransmitter release, then incubated with 10 μM FM4-64FX (Invitrogen) in the presence of 2 μM TTX for 10 min. Cells were then washed twice with HBS + 1 μM TTX, incubated with the quenching reagent SCAS (500 μM ; Invitrogen) in HBS + 1 μM TTX for 4 min, and fixed with 4% PFA/4% sucrose in PBS-MC for 20 min. A parallel set of neurons for each treatment were processed identically, but were used for immunostaining against a structural synaptic marker (bassoon) after fixation. Following imaging (see Experimental Procedures), dendrites were linearized and the density of FM4-64 or bassoon particles determined. (E) Mean (+SEM) normalized (relative to the average control value) density of FM4-64 (black bars) or Bassoon (grey bars) particles in the various treatment groups (21-28 DIV). For the indicated groups (for

FM4-64 and Bassoon, respectively): controls (n = 39, 28 neurons), CNQX alone (n = 40, 26 neurons), TTX alone (n = 40, 30 neurons), TTX + CNQX (n = 40, 29 neurons). AMPAR blockade (CNQX) produced a significant (*p < 0.05, relative to control) increase in FM4-64 uptake that was blocked by coincident AP blockade (TTX+CNQX).



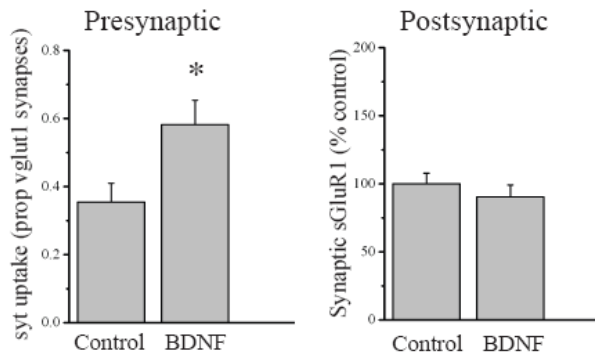
Supplementary Figure 4. Increase in presynaptic function is specific to AMPA receptor blockade. (A) Representative recordings and (B-C) summary of experiments (21-25 DIV) where mEPSCs were recorded under control (untreated) conditions ($n = 17$), or after short term (3 hr) AMPAR blockade (NBQX; $10 \mu\text{M}$; $n = 6$), or NMDAR blockade (APV; $50 \mu\text{M}$; $n = 9$). Mean (+ SEM) mEPSC amplitude (B) and frequency (C) with treatments as indicated. Both AMPAR and NMDAR blockade produce a significant ($* p < 0.05$, relative to control) increase in mEPSC amplitude, but only AMPAR blockade produces a significant increase in mEPSC frequency. (D-E) Neurons (21 DIV) were treated as indicated then live-labeled with a rabbit polyclonal antibody against the luminal domain of synaptotagmin 1 for 5 min in the presence of HBS containing $2 \mu\text{M}$ TTX. (D) Representative examples and (E) mean (+ SEM) syt-lum uptake (DIV 21) in control (untreated; $n = 13$) neurons and neurons treated for 3 hr with NBQX ($10 \mu\text{M}$; $n = 14$; DIV 21) or APV ($50 \mu\text{M}$; $n = 16$). AMPAR blockade significantly ($* p < 0.05$, relative to control) enhanced syt-lum uptake, but NMDAR blockade did not, indicating that rapid compensation in presynaptic function is specific for AMPAR blockade.



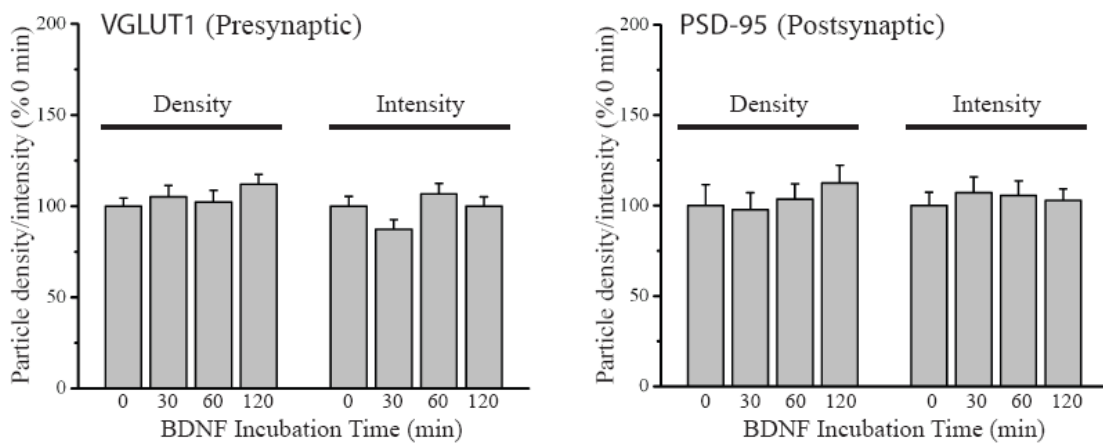
Jakawich et al. Figure S5.

Supplementary Figure 5. Presynaptic and postsynaptic homeostatic changes are induced by AMPAR blockade in parallel (A-C) Neurons (23-27 DIV) were either untreated (control) or treated with CNQX (40 μ M) for 3 hrs prior to washout and subsequent recording of mEPSCs in the presence or absence of 1-Naphthylacetylspermine (Naspm; 10 μ M) to block activity at GluA1 homomeric receptors (see Sutton et al., 2006). Naspm was applied 15-30 min following CNQX washout. (A) Representative recordings and (B-C) summary data from control neurons (n = 14), neurons treated with CNQX (n = 11), control + Naspm (n = 11), or CNQX-treated cells + Naspm (n = 18). (B) Mean (+ SEM) mEPSC amplitude and (C) frequency for each group as indicated. The increase in mEPSC amplitude induced by CNQX treatment (* p < 0.05, relative to control) is abolished by Naspm application. The increase in mEPSC frequency induced by CNQX treatment, however, remains significantly elevated (* p < 0.05, relative to control) even in the presence of Naspm. (D) Representative recordings before and after Naspm (10 μ M) application from the same neuron previously treated with CNQX (3 hr; 40 μ M) (E-F) Summary data of paired recordings (n = 10; 23-27 DIV). (E) The majority (9/10) of CNQX-treated neurons exhibit a decrease in mEPSC amplitude upon the addition of Naspm (left). Mean (+ SEM) mEPSC amplitude in CNQX-treated neurons before and after treatment with Naspm; Naspm produces a significant decrease in mEPSC amplitude (* p < 0.05, paired t-test). (F) A subset of CNQX-treated neurons show a decrease in mEPSC frequency (4/10; left). Mean (+ SEM; right) mEPSC frequency before and after treatment with Naspm; there is a small, but significant (* p < 0.05, paired t-test, one tailed) decrease in mEPSC frequency upon the addition of Naspm, but this diminished mEPSC frequency remains significantly elevated relative to untreated neurons. Dashed line in (E) and (F) indicates average mEPSC amplitude and frequency in untreated controls examined in parallel.

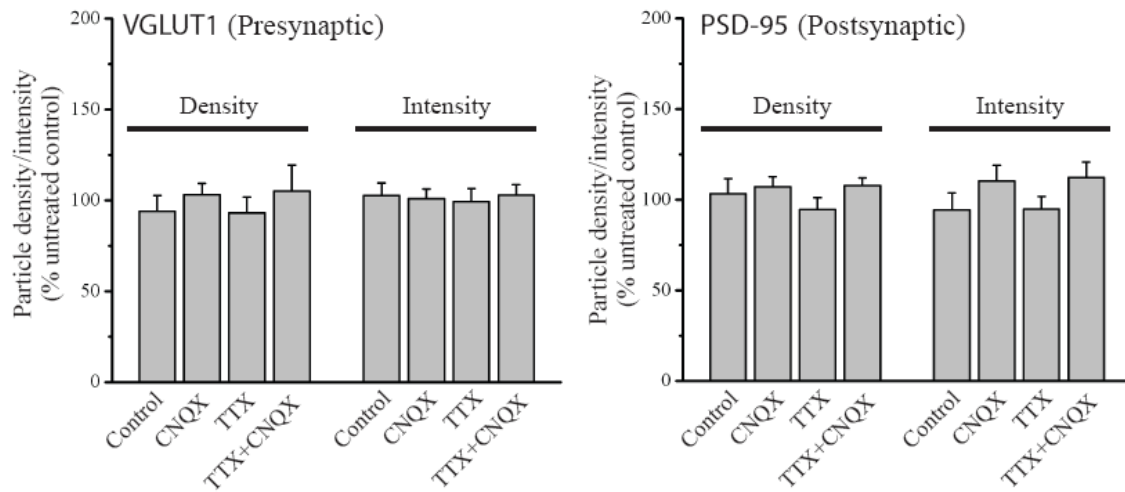
A (Function: + BDNF)



B (Structural: + BDNF)

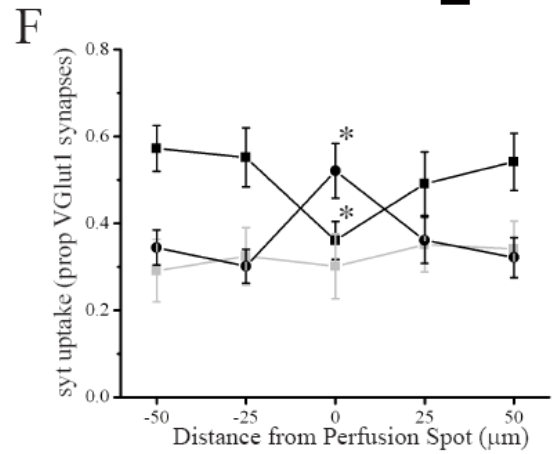
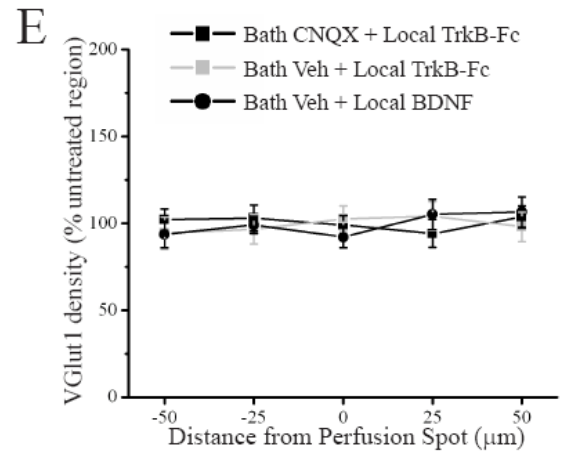
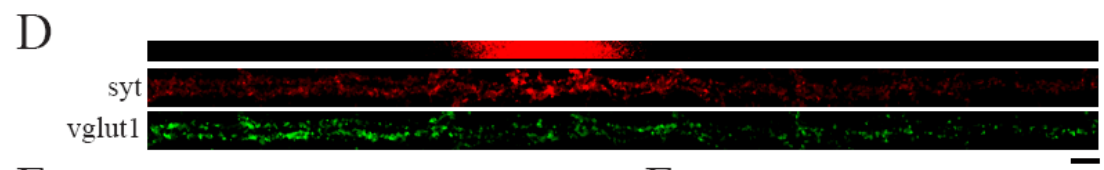
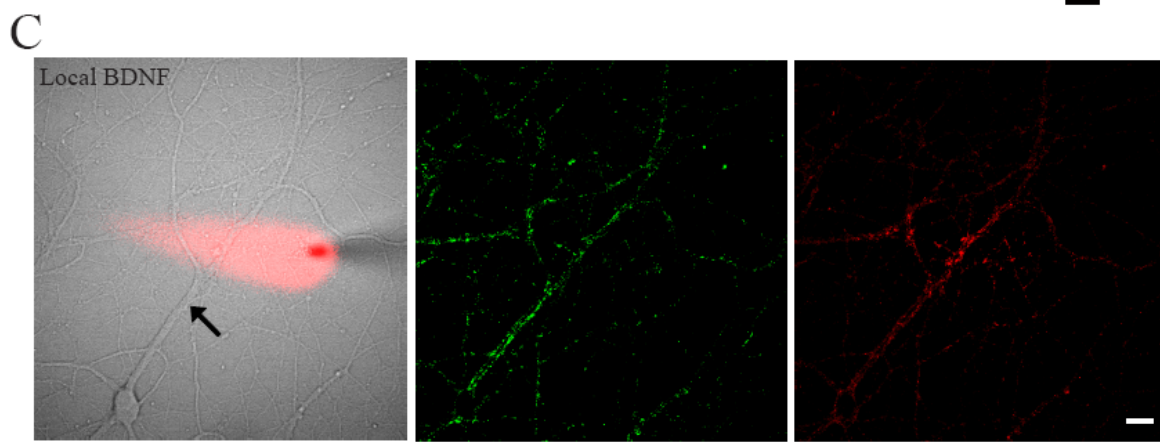
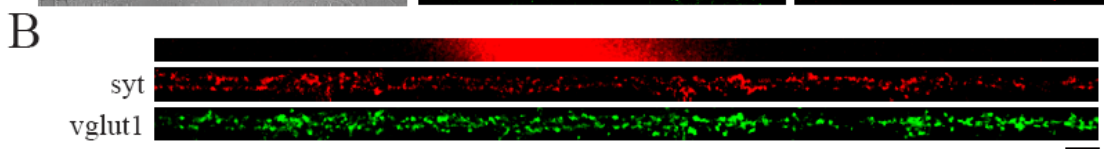
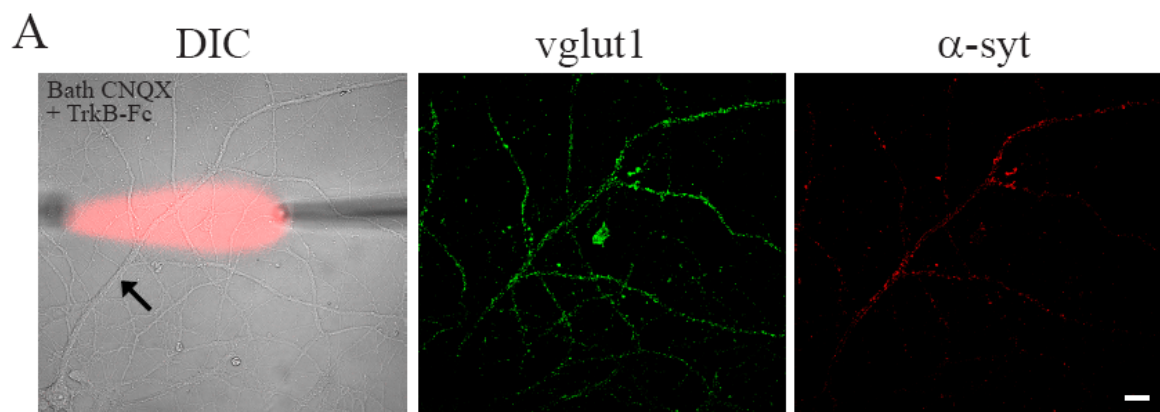


C (Structural: + TrkB-Fc)



Supplementary Figure 6. BDNF alters presynaptic function independent of structural synaptic changes or changes in synaptic AMPARs.

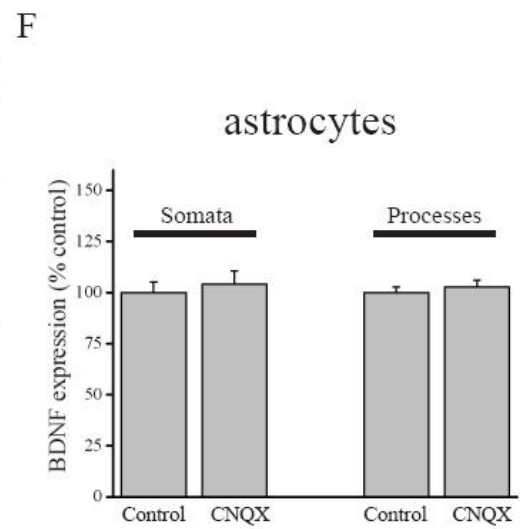
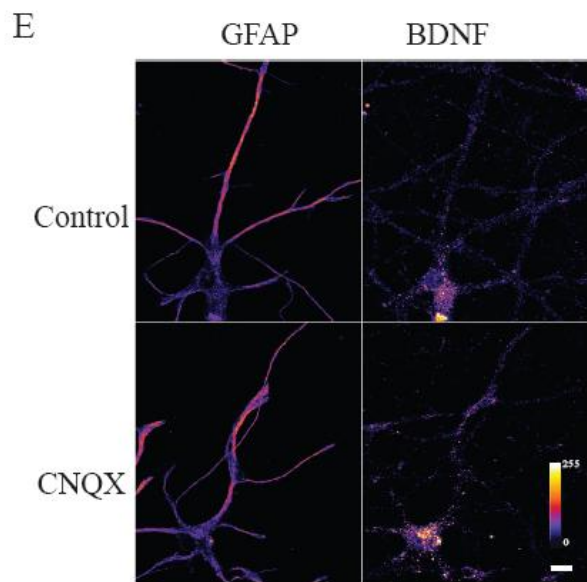
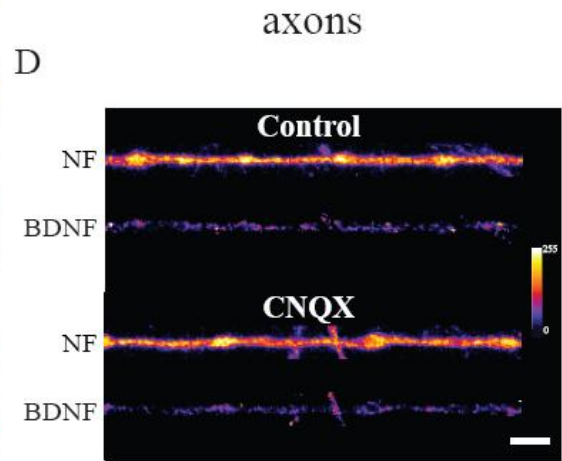
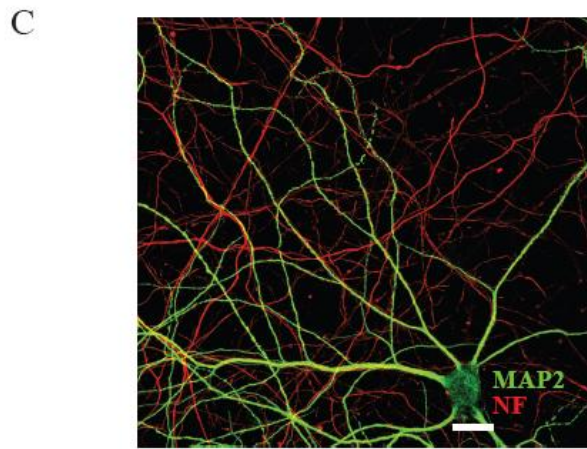
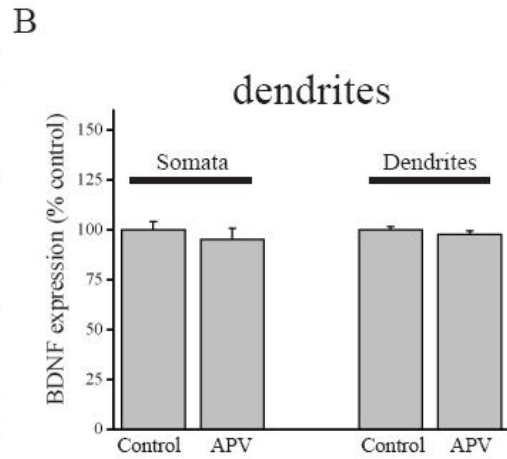
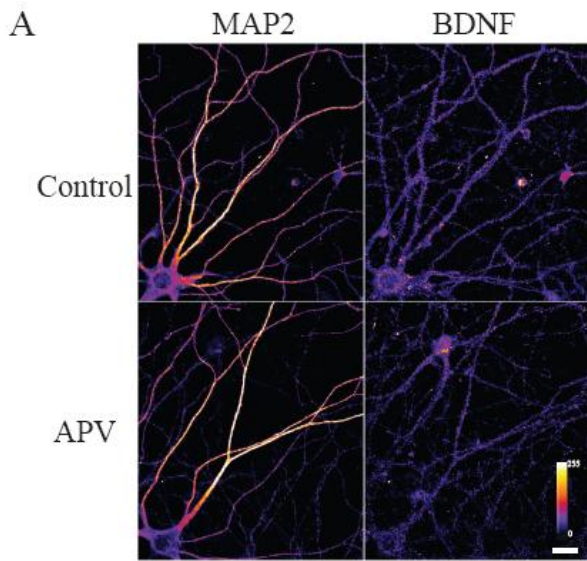
(A) Neurons (21-28 DIV) were either untreated (controls) or treated for 60 min with BDNF (250 ng/ml) prior to live syt-lum uptake (left) or surface GluA1 labeling (right), followed by fixation and staining for vglut1 or PSD-95, respectively. Left, mean (+SEM) proportion of vglut1-positive excitatory presynaptic terminals with corresponding syt-lum signal in control (n = 15) and BDNF-treated neurons (n = 14). Right, mean (+SEM) normalized (% average control value) surface GluA1 expression at excitatory synapses (colocalized GluA1 and PSD95 particles) in control (n = 16) and BDNF-treated neurons (n = 16). BDNF significantly (*p < 0.05, relative to control) enhanced syt-lum uptake at presynaptic terminals, but had no significant effect on surface GluA1 expression at synapses. (B) Mean (+SEM) normalized (relative to 0 min) density and intensity of vglut1 (left) and PSD-95 (right) particles in neurons (25-42 DIV) treated with BDNF (250 ng/ml) for the indicated times. For the groups indicated from left to right in (C), VGLUT1: n = 61, 44, 66, 69 dendrites; PSD-95: n = 17, 16, 15, 18 dendrites. While BDNF produces a significant time-dependent enhancement of presynaptic function (Figure 4), it had no significant effects on the density or intensity of pre- or postsynaptic markers. (C) Mean (+SEM) normalized (relative to untreated control) density and intensity of vglut1 (left) and PSD-95 (right) particles in neurons (DIV 25-28) treated with TrkB-Fc plus the indicated condition; treatments were for 3 hrs. For the groups indicated from left to right in (D), VGLUT1: n = 25, 36, 37, 20 dendrites; PSD-95: n = 21, 20, 23, 30 dendrites. While TrkB-Fc significantly blocks the increase in presynaptic function induced by 3 hr CNQX treatment (Figure 3), it had no significant effects on the density or intensity of pre- or postsynaptic markers in any of the treatment conditions indicated.



Jakawich et al. Figure S7.

Supplementary Figure 7. Local BDNF signaling is necessary and sufficient for homeostatic changes in presynaptic function (A-B) Neurons (21-32 DIV) were perfused with the BDNF scavenger TrkB-Fc (1 $\mu\text{g}/\text{ml}$) for 120 min coincident with either AMPAR blockade (20 μM CNQX to the bath; $n = 9$ dendrites from 6 neurons) or normal activity (bath vehicle; $n = 5$ dendrites from 3 neurons) prior to live labeling with syt-lum as in Figure 2. (A). Representative DIC image showing a CNQX-treated neuron with superimposed TrkB-Fc perfusion spot (red) and the same neuron after live-labeling with syt-lum and retrospective vglut1 immunocytochemistry. (B). Linearized dendrite indicated by the arrow shown in (A) with corresponding syt-lum and vglut1 staining registered to the perfusion area (red). Scale bar = 20 μm and 10 μm in (A) and (B), respectively. A decrease in syt-lum uptake is evident in the area perfused with TrkB-Fc. (C-D) Neurons (21-28 DIV) were perfused with BDNF (250 ng/ml) for 60 min in the presence of normal activity ($n = 8$ dendrites from 5 neurons) prior to live labeling with syt-lum as in Figure 2. (C). Representative DIC image showing a neuron with superimposed BDNF perfusion spot (red) and the same neuron after live-labeling with syt-lum and retrospective vglut1 immunocytochemistry. (D). Linearized dendrite indicated by the arrow shown in (C) with corresponding syt-lum and vglut1 staining registered to the perfusion area (red). Scale bar = 20 μm and 10 μm in (C) and (D), respectively. A local enhancement of syt-uptake is evident in the area perfused with BDNF. (E-F) Analysis of group data from the indicated treatment conditions. On the abscissa, positive and negative values indicate, respectively, segments distal and proximal (towards the soma) from the treated area. (E) Mean (\pm SEM) normalized vglut1 density in treated and un-treated dendritic segments from the indicated groups; all data are expressed relative to the average value in untreated segments. Local perfusion did not affect synaptic density. (F) Mean (\pm SEM) proportion of vglut1-positive

synapses with corresponding syt-lum signal in treated and untreated dendritic segments for the indicated experimental groups. Syt-lum uptake was significantly (* $p < 0.05$, relative to untreated segments) diminished in the area treated with TrkB-Fc in CNQX-treated neurons, but not in vehicle-treated neurons. Conversely, local BDNF application significantly (* $p < 0.05$, relative to untreated segments) enhanced syt-lum uptake in the treated area.



Supplementary Figure 8. Enhanced BDNF expression by AMPAR blockade is specific for the dendritic compartment.

(A) Full-frame examples of MAP2 and BDNF staining in untreated (control) neurons ($n = 41$) or neurons treated for 120 min with 50 μM APV ($n = 40$); scale bar = 20 μm . (B) Mean (+SEM) normalized (relative to the average control value) BDNF expression in either neuron somata (left) or dendrites (right). In contrast to AMPAR blockade, NMDAR blockade did not significantly alter BDNF expression in either compartment.

Experiments were conducted at 21-28 DIV. (C) Full-frame image depicting co-staining for MAP2 (Alexa 488-conjugated goat anti-mouse secondary; green) and neurofilament (NF, using direct Zenon-Alexa 568 conjugation; red), showing non-overlapping dendritic and axonal staining, respectively; scale bar = 20 μm . (D) Representative examples of BDNF staining in axons in both untreated (control) neurons and following 2 hr CNQX treatment; scale bar = 5 μm . AMPAR blockade did not alter BDNF expression in axons (see also, Figure 7F). (E) Full-frame examples of GFAP (left) and BDNF (right) staining from astrocytes (24-36 DIV), in either control ($n = 75$ cells) or CNQX (40 μM , 2 hrs; $n = 86$ cells)-treated cultures; scale bar = 10 μm . (F) Mean (+SEM) normalized (relative to the average control value) BDNF expression in either astrocytic somata (left) or astrocytic processes (right). AMPAR blockade did not significantly alter glial BDNF expression.